H. 知的財産権の出願・登録状況

1．特許取得　　該当無し

2．実用新案登録　　該当無し

3．その他　　該当無し

I. 参考文献

1. Sutter TR, et al. J Biol Chem 1994;269:13092-9.

2. Shimada T, et al. Cancer Res 196;56:2979-84.

3. Hayes C, et al. Proc Natl Acad Sci USA 1996;93:9776-81.

4. Spink D, et al. J Steroid Biochem Mol Biol 1997;62:223-32.

5. Lee AJ, et al. Endocrinology 2003;144:3382-98.

6. Han X, et al. Carcinogenesis 1994;15:997-1000.

7. Newbold RR, et al. Cancer Res 2000;60:235-7.

8. Murray GI, et al. Cancer Res 1997;57:3026-33.

9. Bartel DP. Cell 2004;116:281-97.

10. Cheung YL, et al. Cancer Lett 1999;139:199-205.

11. Ragavan N, et al. Cancer Lett 2004;215:69-78.

12. Tsuchiya Y, et al. J Biochem 2003;133:583-92.

13. Tsuchiya Y, et al. Cancer Res 2004;64:3119-25.

14. Tsuchiya Y, et al. J Biochem 2006;139:527-34.

15. Shehin SE, et al. J Biol Chem 2004;275:6770-6.

16. Zhang L, et al. J Biol Chem 1998;273:5174-83.

17. Zheng W, et al. Mol Pharmacol 2005;67:499-512.

18. Lu J, et al. Nature 2005;435:834-8.

19. Calin GA, et al. Proc Natl Acad Sci USA 2004;101:2999-3004.

20. Carnell DM, et al. Int J Radiat Oncol Biol Phys 2004;58:500-9.

21. Stoilov I, et al. Am J Hum Genet 1998;62:573-84.

22. Bejjani BA, et al. Hum Mol Genet 2000;9:367-74.

23. Libby RT, et al. Science 2003;299:1578-81.

別紙４

研究成果の刊行に関する一覧表

雑誌

発表者氏名	論文タイトル名	発表誌名	巻号	ページ	出版年
Keiichi Minami, Rawiwan Maniratanachote, Miki Katoh, Miki Nakajima and Tsuyoshi Yokoi	Simultaneous measurement of gene expression for hepatotoxicity in thioacetamide-administered rats by DNA microarrays	Mutation Research	603	64-73	2006
Yuki Tsuchiya, Miki Nakajima, Shingo Takagi, Miki Katoh, Wenchao Zheng, Colin R Jefcoate, and Tsuyoshi Yokoi	Binding of steroidogenic factor-1 to the regulatory region might not be critical for transcriptional regulation of the human CYP1B1 gene.	Journal of Biochemistry	139	527-534	2006
Raiwan Maniratanachote, Keiichi Minami, Miki Katoh, Miki Nakajima, and Tsuyoshi Yokoi	Dephosphorylation of ribosomal protein P0 in response to troglitazone-induced cytotoxicity	Toxicology	166	189-199	2006
Yuki Tsuchiya, Miki Nakajima, Shingo Takagi, Takao Taniya, and Tsuyoshi Yokoi	MicroRNA regulates the expression of human cytochrome P450 1B1	Cancer Research	66	9090-9098	2006
Yusuke Hara, Miki Nakajima, Ken-ichi Miyamoto and Tsuyoshi Yokoi	Morphine glucuronoxyltransferase activity in human liver microsomes is inhibited by a variety of drugs that are co-administered with morphine	Drug Metabolism and Pharmacokinetics		印刷中	2007
Rawiwan Maniratanachote and Tsuyoshi Yokoi	A mechanistic view of troglitazone hepatotoxicity	Jouranal of Applied Toxicology		印刷中	2007

Available online at www.sciencedirect.com
SCIENCE DIRECT
ELSEVIER
Mutation Research 603 (2006) 64–73
Genetic Toxicology and Environmental Mutagenesis
www.elsevier.com/locate/gentox
Community address: www.elsevier.com/locate/mutres

Simultaneous measurement of gene expression for hepatotoxicity in thioacetamide-administered rats by DNA microarrays

Keiichi Minami, Rawiwan Maniratanachote, Miki Katoh, Miki Nakajima, Tsuyoshi Yokoi *

Drug Metabolism and Toxicology, Division of Pharmaceutical Sciences, Graduate School of Medical Science, Kanazawa University, Kanazawa 920-1192, Japan

Received 26 August 2005; received in revised form 26 September 2005; accepted 28 October 2005
Available online 5 December 2005

Abstract

DNA microarray technology was developed as a tool for simultaneously measuring a number of gene expression changes, and has been applied for investigations of toxicity assessments of chemicals. In this study, we used a typical hepatotoxicant, thioacetamide (TA), to find correlations between the extent of hepatotoxicity and certain gene expression patterns or specific gene expression profiles. TA was intraperitonealy administered at high (400 mg/kg), medium (150 mg/kg) or low (50 mg/kg) dose (four rats per group) and then the serum and liver were collected at the indicated time (6, 12, 24, 36 and 48 h). Serum biochemical markers were measured and hepatic mRNA expression profiles were analyzed by a DNA microarray. Serum aspartate aminotransferase (AST) and alanine aminotransferase (ALT) were increased by TA-administration in a dose-dependent manner and reached the maximum at 24 h. Hierarchical clustering analysis of all dosage groups revealed in 2 major clusters, distinguished by an early (6 and 12 h) and a late (24, 36 and 48 h) phase. The early and late phase clusters were sorted in time- and dose-dependent manners. The major gene expression profile obtained by quality-threshold (QT) clustering analysis showed the same maximal toxic time as that estimated by the serum biochemical markers. The individual expression profiles of the candidate genes selected in our previous studies and the simultaneous gene expression patterns measured by five typical hepatotoxicants including TA also reflected the hepatotoxicity of TA. These findings suggest that the potential toxic effects appearing as gene expression changes are independent of the dosage of TA. This study suggested that the major gene expression profile estimated by QT clustering would be a sensitive marker of hepatotoxicity.

Keywords: Gene expression profiles; Hepatotoxicity; DNA microarray

1. Introduction

The prediction of chemical-induced adverse effects on an organism is one of the aims of toxicology. In the past several years, a microarray technology has rapidly developed. Microarrays are available to assess both known and unknown genes in the experimental materials. Microarrays are also available to assess simultaneously the effects of various factors on the gene expression of all known sequences including expression sequence tags (ESTs) at the RNA level.

For microarray data assessment, several clustering methods are often used. Clustering places the data of interest into a small number of relatively homo-

* Corresponding author. Tel.: +81 76 234 4407; fax: +81 76 234 4407.
E-mail address: TYOKOI@kenroku.kanazawa-u.ac.jp (T. Yokoi).

1383-5718/$ – see front matter © 2005 Elsevier B.V. All rights reserved.
doi:10.1016/j.mrgentox.2005.10.008

geneous groups or clusters [1]. For example, there is hierarchical clustering expressed by a dendrogram, *K*-means clustering [2], and quality-threshold (QT) clustering [3]. These clustering methods are useful ways to extract and visualize one-to-one correlations. Microarray technology can be used as a tool for clarifying the mechanisms of chemical-induced toxicity, forecasting the adverse effects of drug candidates and improving the process of risk assessment and safety evaluation.

The liver is one of the first organs to be exposed when chemicals are administered perorally or via the portal vein. Chemical concentrations in the liver are often much higher than the peak plasma concentration. The liver is also the major site for metabolizing xenobiotics and these chemicals can lead to the formation of active metabolites. Thus, the liver is one of the primary targets for various types of chemical-induced toxicity. Therefore, investigating the gene expression changes and comparing the gene expression profiles to the extent of liver toxicity are useful for the assessment of liver toxicity.

To construct an animal model of liver toxicity, we chose thioacetamide (TA) as a potent hepatotoxicant that requires metabolic activation by mixed-function oxidases. TA is metabolized by cytochrome P450 (CYP) 2B, CYP2E1 and flavin-containing monooxygenase (FMOs) to its toxic metabolites [4,5] and these intermediate metabolites might bind to cellular proteins by the formation of acetylimidolysine derivatives [6]. The reactive metabolites responsible for TA hepatotoxicity are the radicals derived from thioacetamide-*S*-oxide and the reactive oxygen species derived as subproducts in the process of microsomal TA oxidation, both of which deplete reduced glutathione leading to oxidative stress [7–11].

The purpose of the present study is to determine the correlations between biochemical markers for hepatotoxicity and hepatic gene expression profiles at various doses of TA-administration in rats, and then to extrapolate the DNA microarray data for predicting hepatotoxic chemicals.

2. Materials and methods

2.1. Animals and chemicals

Male Sprague–Dawley rats (5-week old, 130–150 g) were obtained from SLC Japan (Hamamatsu, Japan). Animals were housed in the institutional animal facility in a controlled environment (temperature 25 ± 1 °C, humidity 50 ± 10% and 12 h light/12 h dark cycle) with access to food and water ad libitum. Animals were acclimatized for a week before use. Animal maintenance and treatment were conducted in accordance with the National Institutes of Health Guide for Animal Welfare of Japan, as approved by the Institutional Animal Care and Use Committee of Kanazawa University. TA (CAS No. 62-55-5) was obtained from Wako Pure Chemical Industries (Osaka, Japan). ISOGEN, RNA extraction reagent, was purchased from Nippon Gene (Tokyo, Japan). CodeLink™ Expression Assay Reagent kit, Manual Prep and streptavidin-Cy5 were from GE Healthcare Amersham Biosciences (Buckinghamshire, UK). The QIAquick PCR purification kit and a RNeasy mini kit were from Qiagen (Hilden, Germany). NEN Blocking Reagent and Biotin 11-UTP were from Perkin-Elmer Life Sciences (Boston, MA). ReverTra Ace (Moloney Murine Leukemia Virus Reverse Transcriptase RnaseH Minus) was from Toyobo (Tokyo, Japan). Random hexamer and SYBR® Premix Ex Taq™ (perfect real time) were from Takara (Osaka, Japan). All primers were commercially synthesized at Hokkaido System Sciences (Sapporo, Japan). Other chemicals were of the highest grade commercially available.

2.2. TA-administration and assessment of liver injury

Sixty-four rats were assigned to 16 groups (four rats/group). Rats received a single dose of TA dissolved in saline by intraperitoneal injection. The dosing solutions were prepared to deliver a volume of 2 ml/kg as follows; 400 mg/kg high dose, 150 mg/kg medium dose, 50 mg/kg low dose. At the indicated time (6, 12, 24, 36, and 48 h after the administration), blood samples were collected from the atrium, and then the rats were sacrificed and the liverscollected. Four typical biochemical markers for hepatotoxicity (aspartate aminotransferase, AST; alanine aminotransferase, ALT; lactate dehydrogenase, LDH; bilirubin) were measured by SRL (Tokyo, Japan).

2.3. RNA isolation

Total hepatic RNA was isolated using ISOGEN. Approximately 100 mg of whole liver were lysed with 1.0 ml of the reagent. Chloroform (200 μl) was added and vortexed vigorously for 15 s. The mixture was centrifuged at 15,000 × *g* for 15 min at 4 °C. The aqueous phase was transferred carefully to a new tube, and the RNA was precipitated with 0.5 ml of isopropyl alcohol for 10 min at room temperature. The mixture was centrifuged at 15,000 × *g* for 10 min. After washing with 75% ethanol, the pellet was dissolved in diethylpyrocarbonate-treated water. Equal amounts of total mRNA from samples of each administration were pooled and used for the microarray analysis and real-time reverse transcriptase (RT)-PCR.

2.4. Microarray analysis

Microarray experiments were performed using a CodeLink™ Bioarray Perfect System according to the manufacturer's protocol (GE Healthcare Amersham Biosciences). In this experiment, we used Codelink™ Uniset Rat

I Bioarray (GE Healthcare Amersham Biosciences) consisting of 9936 genes including ESTs. Processed slides were scanned with an Agilent G2565BA Microarray Scanner using Agilent Scan Control Software (Agilent Technologies, Palo Alto, CA) with the laser set to red (633 nm) and the photomultiplier tube (PMT) value to 70%. The scanned images for each slide were analyzed using the CodeLink™ Expression Analysis Software (GE Healthcare Amersham Biosciences). The microarray data quality control was as follows: present, no flags (neither marginal nor absent); marginal, low quality spots judged by analysis software; absent, low signal density spots.

2.5. Real-time RT-PCR

Rat V1a arginine vasopressin receptor (Avpr1a), cyclin G1 (Ccng1), growth arrest and DNA-damage-inducible 45alpha (Gadd45a), heme oxygenase 1 (Hmox1), L-3-hydroxyacyl-Coenzyme A dehydrogenase (Hadhsc), lysozyme (Lyz), sulfotransferase 1a2 (Sult1a2), T-cell death associated gene (Tdag) and GAPDH were quantified by real-time RT-PCR. Primer sequences used in this study were as follows: Avpr1a: 5′-TAC GTG ACC TGG ATG ACC AG-3′ and 5′-AGC AAC GCC GTG ATT GTG AT-3′ [12], Ccng1: 5′-CCT TCC AAT TTC TGC AGC TC-3′ and 5′-CTT GGA AAC AAG CTC TTG CC-3′ [13], Gadd45a: 5′-AAG ATC GAA AGG ATG GAC ACG-3′ and 5′-GTA GCA ACA GCT CTG CCA GC-3′ [14], Hmox1: 5′-ATA GAG CGA AAC AAG CAG A-3′ and 5′-TAG AGC TGT TTG AAC TTG G-3′, Hadhsc: 5′-TGC AGA TCA CAA ACA TAG CC-3′ and 5′-TCC AGT CCA ACA TAG TCA AG-3′, Lyz: 5′-CTC AAA CCA ACA GGG CTT TC-3′ and 5′-CCC AAG ATC AAC TCG TCT CC-3′ [15], Sult1a2: 5′-TCA TTG AGT GGA CTT TGC CTT-3′ and 5′-CAC TTT TCC AGC TTT GAA CTG-3′, Tdag: 5′-CCA AGC AGG TAC AAC ATC AG -3′ and 5′-TTC TGC CTC GTA GAC TTG AC-3′, GAPDH: 5′-GTT ACC AGG GCT GCC TTC TC-3′ and 5′-GGG TTT CCC GTT GAT GAC C-3′. For RT process, total RNA (4 μg) and 150 ng random hexamer were mixed and incubated at 70 °C for 10 min. The RNA solution was added to a reaction mixture containing 100 units of ReverTra Ace, reaction buffer and 0.5 mM dNTPs in a final volume of 40 μl. The reaction mixture was incubated at 30 °C for 10 min, 42 °C for 1 h and heated at 98 °C for 10 min to inactivate the enzyme. Real-time PCR was performed using the Smart Cycler® (Cepheid, Sunnyvale, CA) with Smart Cycler® software (Ver. 1.2b). The PCR mixture contained 1 μl of template cDNA, SYBR® Premix Ex Taq™ solution and 10 pmol of sense and antisense primers. The PCR condition for Ccng1, Sult1a2 and GAPDH was as follows: after an initial denaturation at 95 °C for 30 s, the amplification was performed by denaturation at 94 °C for 4 s, annealing and extension at 64 °C for 20 s for 45 cycles. The PCR condition for other six genes was as follows: after an initial denaturation at 95 °C for 20 s, the amplification was performed by denaturation at 95 °C for 5 s, annealing at 55 °C for 10 s and extension at 72 °C for 15 s for 45 cycles. The amplified products were monitored directly by measuring the increase of the dye intensity of the SYBR® Green I.

2.6. Data management

Microarray data management was performed with GeneSpring software (Agilent Technologies). Comparison of present genes, fold change determinations, experiment normalization and various clustering analyses were performed. The gene expression values for each array were normalized to their respective median value. All clustering analyses were performed using standard correlations. Fold change filters included the requirement that the genes be present in at least 200% of controls for up-regulated genes and lower than 50% of controls for down-regulated genes.

3. Results

3.1. Assessment of liver toxicity

The serum biochemical markers in the TA-administered groups were measured at 6, 12, 24, 36 and 48 h after administration (Fig. 1). The AST activities of all dosage groups were significantly high at 24 h. The changes of ALT activities were similar to those of the AST activities. The LDH activity increased significantly in the medium dose- and the high dose-administered groups at 24 h, but not in the low dose-administrated groups. No significant change of the unconjugated bilirubin was observed in any of the groups (data not shown), whereas conjugated bilirubin increased only in the 24 h high-dose group (0 h: 0 mg/dl, 24 h: 0.3 mg/dl). Taking these results into consideration, the maximal toxic times of each TA dosage were estimated as 24 h.

3.2. Two-way hierarchical clustering of gene expression profiles in TA-induced hepatotoxicity in rats

The mRNA expression profiles in the three dosage and five time points were determined using the data from the DNA microarray. Two-way hierarchical clustering was performed based on the expression profiles of the genes with a significant variation in the expression level across all the experiments. After cutting off the absent and marginal flags, 7978 out of 9936 genes were present in this experiment. The results are shown in a color-coded matrix (Fig. 2) where samples are ordered on the horizontal axis and genes on the vertical axis on the basis of the similarity of their expression profiles.

The administered groups were sorted into two large clusters that extensively differed with respect to an early phase (6 and 12 h; left cluster) or a late phase (24, 36 and 48 h; right cluster) (Fig. 2A). In the early phase cluster,

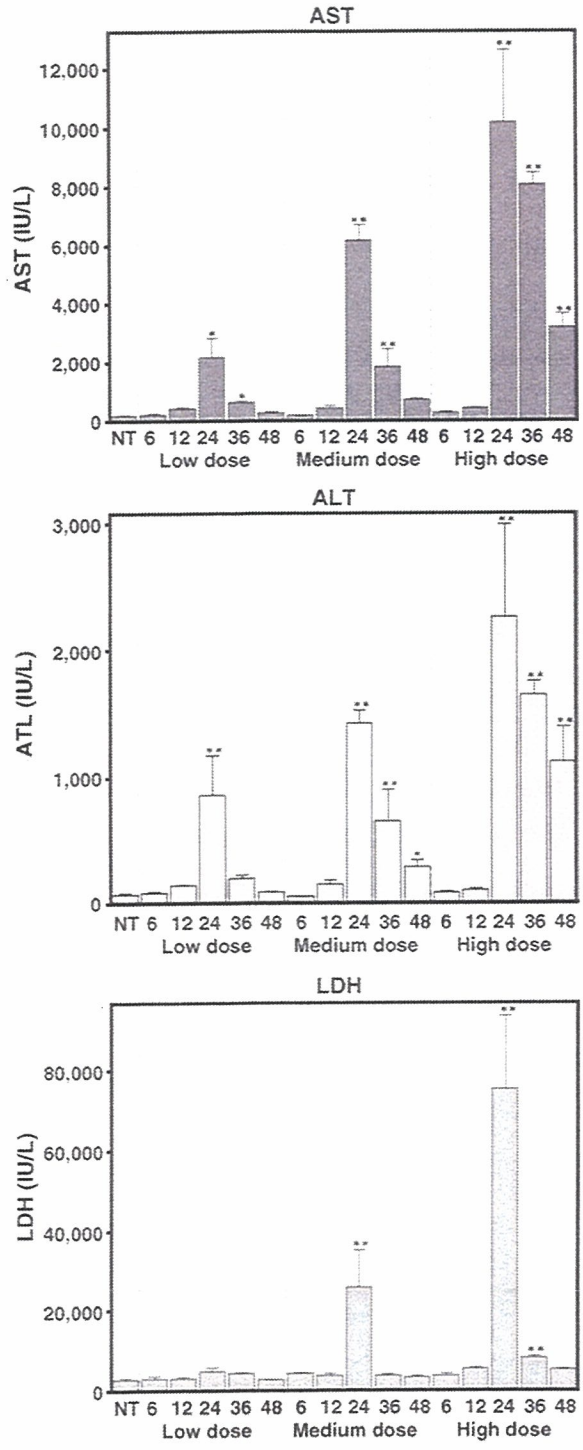

Fig. 1. Changes of AST, ALT and LDH in serum of TA-administered rats. TA was administered at high dose (400 mg/kg weight), medium dose (150 mg/kg weight) and low dose (50 mg/kg weight). Blood samples were collected at 6, 12, 24, 36, 48 h after administration. Data are expressed as mean ± S.E. from four rats. Significantly different from NT group ($^{*}p < 0.05$, $^{**}p < 0.01$). NT; non-treated.

Table 1
Classification of genes those expression were significantly changed in all TA-administered groups

Category	Total[a]	Present[b]	Up (%)	Down (%)
Apoptosis regulator	33	25	4 (16.0)	0 (0)
Cancer	51	28	3 (10.7)	0 (0)
Cell cycle regulator	25	19	2 (10.5)	1 (5.3)
Chaperone	33	19	1 (5.3)	2 (10.5)
Enzyme	852	657	24 (3.7)	100 (15.2)
Immunity protein	42	31	0 (0)	2 (6.5)
Microtublar protein	16	8	0 (0)	1 (12.5)
Nucleic acid binding	175	126	12 (9.5)	6 (4.8)
Other groups	102	71	2 (2.8)	1 (1.4)
RNA	2	1	0 (0)	0 (0)
Signal transducer	201	124	7 (5.6)	9 (7.3)
Storage	3	2	0 (0)	0 (0)
Structural protein	181	116	7 (6.0)	12 (10.3)
Transport	313	208	10 (4.8)	26 (12.5)
Total	2029	1435	72 (5.0)	160 (11.1)

Up-regulated gene showed more than 200% expression of control. Down-regulated gene showed less than 50% expression of control.
[a] Gene number those category were defined.
[b] Gene number showing enough spot density.

the 12 h-groups were sorted into small hierarchies. On the other hand, the late phase cluster groups were sorted in a dose-dependent manner except for the 24 h-group. Especially, all dosages in the 24 h-groups were categorized at the same level.

We also performed hierarchical clustering based on each dosage (Fig. 2B). The clusters were sorted in a similar pattern as shown in Fig. 2A. The distance between the early (6 and 12 h) and the late (24, 36 and 48 h) phase was increased in a time-dependent manner as shown in the dendrogram of each group (above the matrix, Fig. 2B).

3.3. *Category classification of genes in TA-induced hepatotoxic Rats*

To evaluate the gene expression pattern on the basis of gene function, we classified the genes whose expressions were significantly changed at all dosages in the 24 h groups (Table 1). Based on each gene annotation, 13 categories were classified. Based on the percentage and the gene numbers categorized by gene annotation, the genes in the apoptosis regulator and the nucleic acid binding category were typically up-regulated and the genes in the enzyme, structural protein and transport category were down-regulated (Table 1).

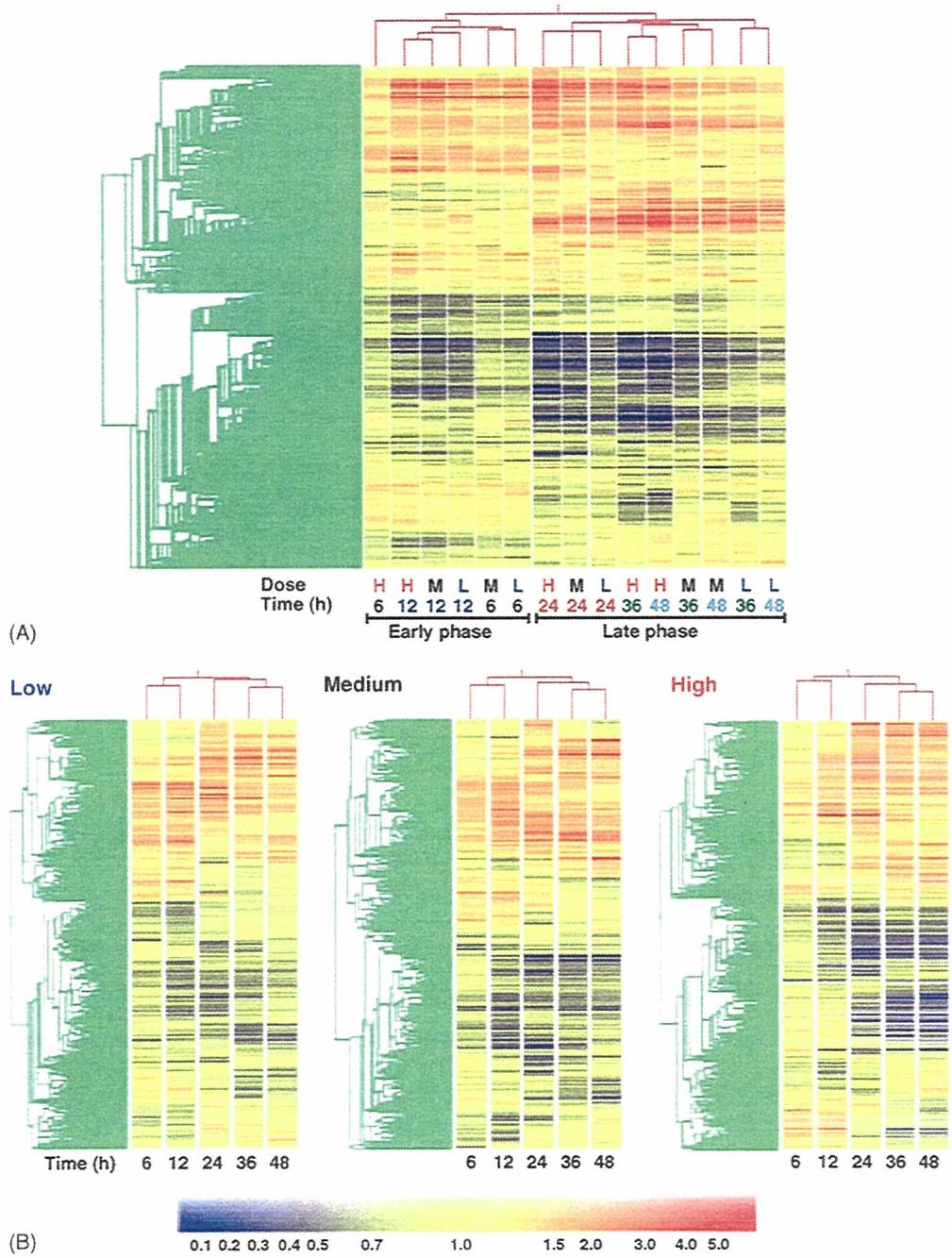

Fig. 2. Two-way hierarchical clustering analyses of hepatic gene expression profiles. Hierarchical clustering of all groups (A) and each dosage group (B). Data of 7978 genes are expressed in a color-coded matrix. Red- and blue-color in matrix indicate the expression levels of above and below the median, respectively. Dendrograms of each group (above the matrix, red lines) and gene (left of the matrix, green lines) represent the overall similarities in gene expression profiles. H: high dose (400 mg/kg); M: medium dose (150 mg/kg); L: low dose (50 mg/kg).

3.4. QT clustering analysis based on the dose of TA

QT clustering analysis was performed in order to estimate the major gene expression profiles based on the TA dosage (Fig. 3). In this process, we used GeneSpring QT clustering algorism. In all dosage groups, we selected the highest correlation coefficient that identified both the up- and the down-regulated types of cluster. The analysis setting for the minimal cluster size was 1000 genes and the minimal correlation coefficients of the 6, 12, 24, 36, and 48 h groups were 0.82, 0.92, 0.91, 0.88 and 0.86, respectively. The probe sets used in this clustering were the same as those used in the hierarchical clustering (7978 of 9936 genes). In the up-regulated

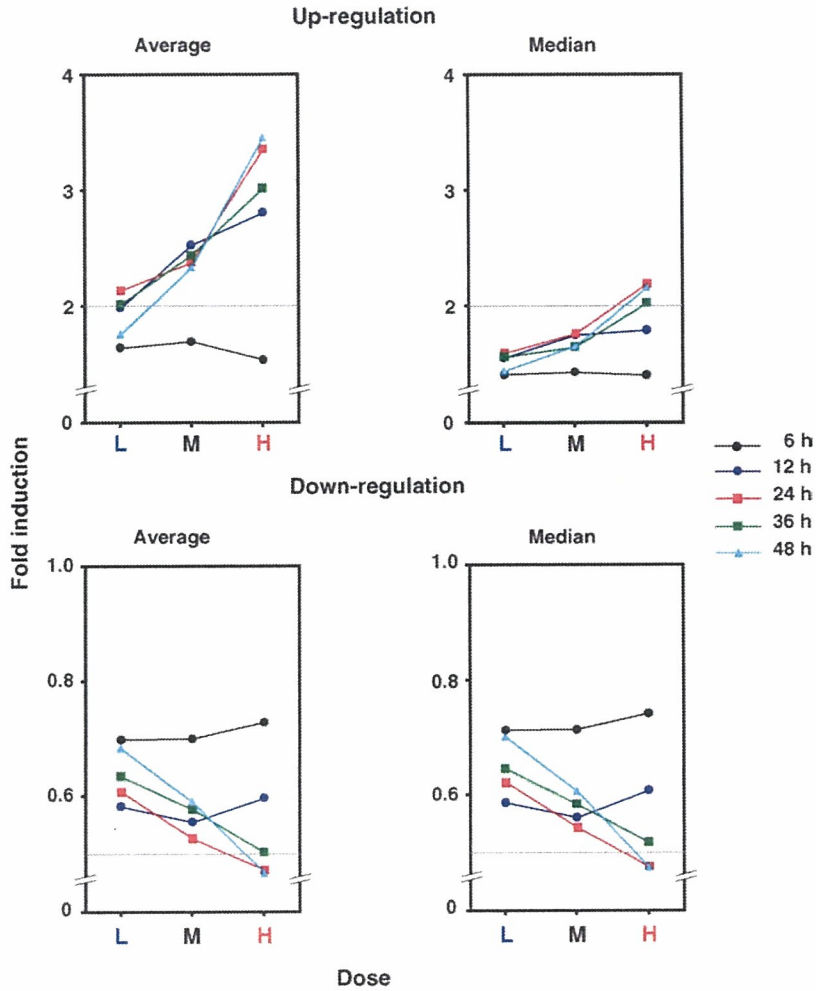

Fig. 3. QT clustering analyses based on the dose of TA. Groups at 6, 12, 24, 36, and 48 h after administration were evaluated and expressed as average (left) or median (right) values. Analysis settings are described in Section 3. Minimal correlation coefficients selected in this analysis were as follows: 6 h, 0.82; 12 h, 0.92; 24 h, 0.91; 36 h, 0.88; 48 h, 0.86. H: high dose; M: medium dose; L: low dose.

cluster, the gene numbers of each time group were as follows: 6 h, 1028; 12 h, 1010; 24 h, 1003; 36 h, 1008; 48 h, 1000. In the down-regulated cluster, the gene numbers of each time group were as follows: 6 h, 1903; 12 h, 1724; 24 h, 1546; 36 h, 1533; 48 h, 1513. The expression changes of these genes in each dosage group are shown as average and median values (Fig. 3). As a result, both the average and the median of the gene expression profiles before 12 h showed no difference between the three dosage groups. However, the gene expression profiles after 24 h of administration changed in a dose-dependent manner.

3.5. QT clustering analysis based on the time after TA-administration

QT clustering analysis was performed in order to estimate the major gene expression profiles based on the time after TA-administration (Fig. 4). In the low-limited correlation analysis, we selected the highest correlation coefficient that identified the up- and down-regulated type of clusters. The low-limited analysis setting for the minimal cluster size was 1000 genes and the minimal correlation coefficients of the low-, medium- and high-dose groups were 0.68, 0.58, and 0.47, respectively. The probe sets used in this clustering were the same as those used in the hierarchical clustering (7978 of 9936 genes). In the up-regulated type cluster, the low-, medium- and high-dose groups contained 1021, 1003 and 1000 genes, respectively (Fig. 4A). The down-regulated type cluster of the low-, medium- and high-dose groups contained 2129, 2050 and 1606 genes, respectively (Fig. 4B). In the high-limited correlation analysis, we selected the highest correlation coefficient that identified only one dominant cluster (Fig. 4C). The high-limited correlation analysis setting for the minimal cluster size was 1000 genes and

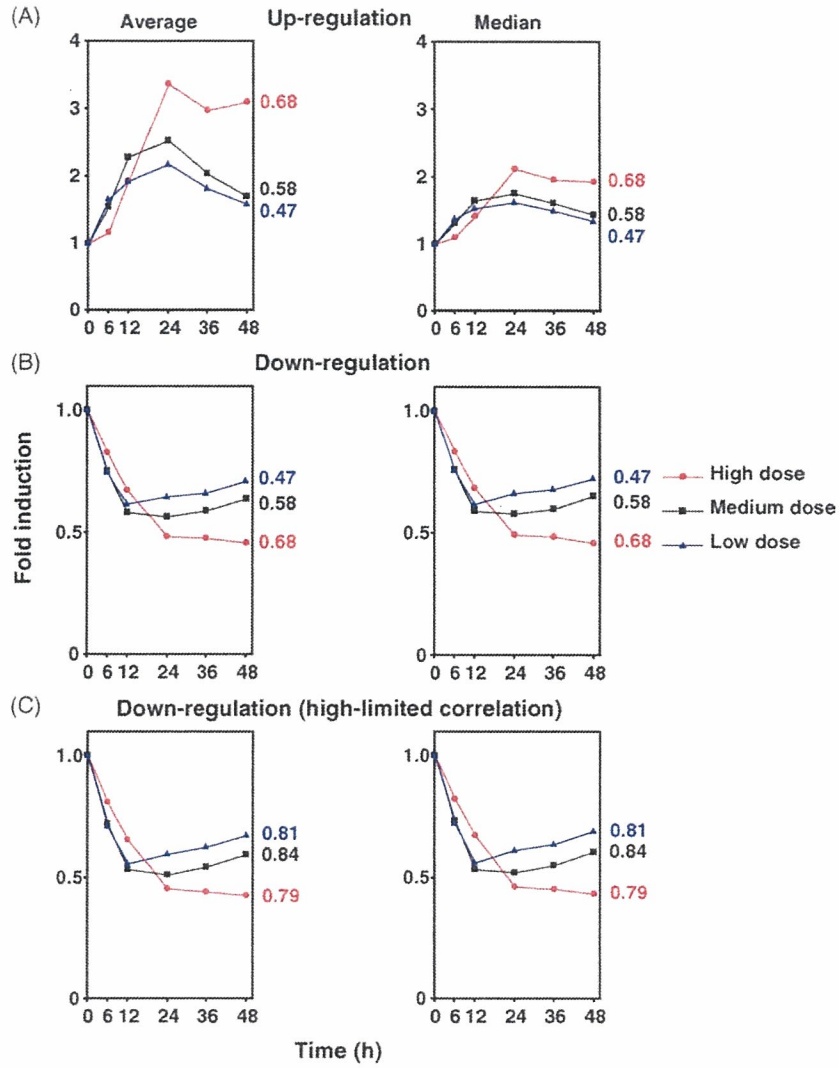

Fig. 4. QT clustering analyses based on the time after TA-administration. Groups at 6, 12, 24, 36, and 48 h after administration were evaluated with low (A and B)- and high (C)-limited correlation coefficients. Analysis settings are described in Section 3. Data are expressed as average or median values of these clusters. The minimal correlation coefficients selected in this analysis were as follows: low-limited correlation: high dose, 0.68; medium dose, 0.58; low dose, 0.47 (A and B). High-limited correlation: high dose, 0.79; medium dose, 0.84; low Dose, 0.81 (C).

the minimal correlation coefficients of the low-, medium- and high-dose groups were 0.79, 0.84 and 0.81, respectively (Fig. 4C). In the down-regulated type cluster, the low-, medium- and high-dose groups contained 1016, 1002 and 1016 genes, respectively (Fig. 4C). Both the average and median values of the QT clustering and the expression profiles of almost all dosage groups demonstrated peak values at 24 h after administration, which was the same as the maximal toxic time. Independently of the extent of toxicity, the major gene expression profiles based on the time after TA-administration showed almost the same pattern. However, the changes of the up- and down-regulated genes occurred in a dose-dependent manner.

3.6. Toxicity marker analysis

Previously, in rats we identified potential hepatotoxic marker genes from five hepatotoxicants (acetaminophen, bromobenzene, carbon tetrachloride, dimethylnitrosamine and TA) by using cDNA microarray [16]. The up- and down-regulated groups consisted of nine and seven genes, respectively (Fig. 5). In the present study, changes in the expression of potential hepatotoxic marker genes were demonstrated. As shown in Fig. 5, the maximal up- or down-regulated time points in almost all the individual gene expression profiles reflected the maximal toxic time. In addition, the individual gene expression profiles of each dosage showed similar patterns. In

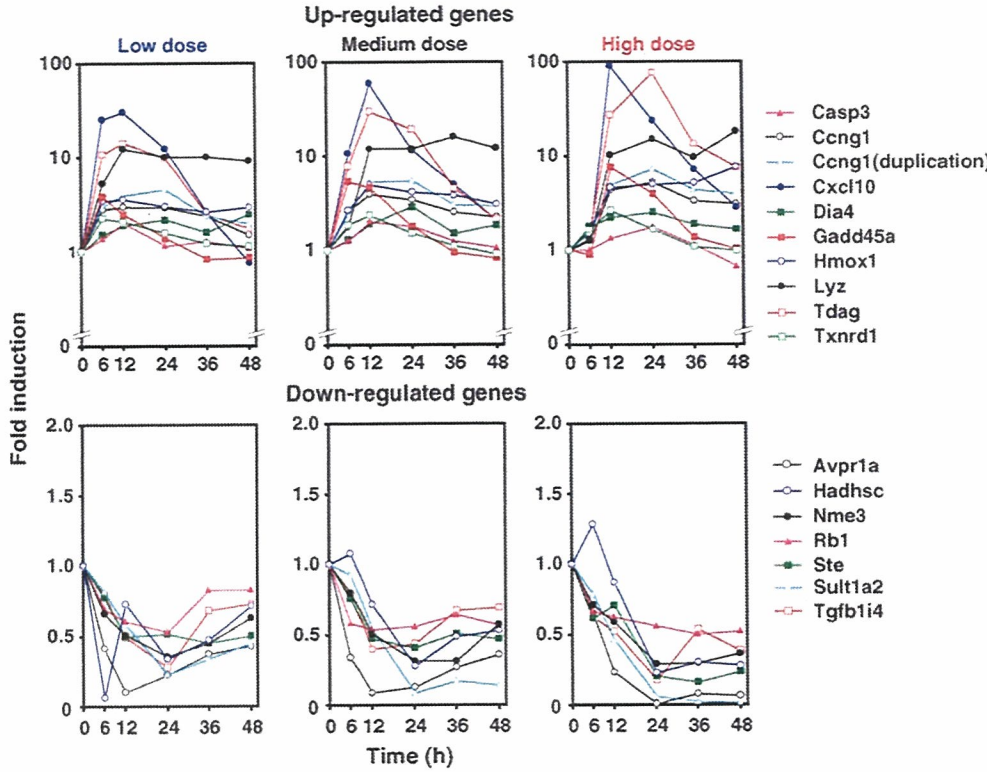

Fig. 5. Gene expression profiles of the selected genes. The up-regulated group consisted of nine genes and the down-regulated group seven genes. Total RNA samples from four rats were pooled and used for this analysis. Symbols, accession numbers and gene names are as follows: Casp3, NM_012922, caspase 3, apoptosis related cysteine protease (ICE-like cysteine protease) mRNA; Ccng1, NM_012923, cyclin G1 mRNA; Cxcl10, U22520, interferon inducible protein 10 (IP-10) mRNA, complete cds; Dia4, NM_017000, diaphorase (NADH/NADPH) mRNA; Gadd45a, NM_024127, growth arrest and DNA-damage-inducible 45 alpha mRNA; Hmox1, NM_012580, heme oxygenase (decycling) 1 mRNA; Lyz, NM_012771, lysozyme mRNA; Tdag, NM_017180, T-cell death associated gene mRNA; Txnrd1, NM_031614, thioredoxin reductase 1 mRNA; Avpr1a, Z11690, mRNA for V1a arginine vasopressin receptor; Hadhsc, NM_057186, L-3-hydroxyacyl-coenzyme A dehydrogenase, short chain mRNA; Nme3, NM_053507, expressed in non-metastatic cells 3, protein (nucleoside diphosphate kinase) mRNA; Rb1, D25233, mRNA for retinoblastoma protein, partial sequence; Ste, NM_012883, sulfotransferase, estrogen preferring mRNA; Sult1a2, NM_031732, sulfotransferase family 1A, member 2 mRNA; Tgfb1i4, NM_013043, transforming growth factor beta 1-induced transcript 4 mRNA.

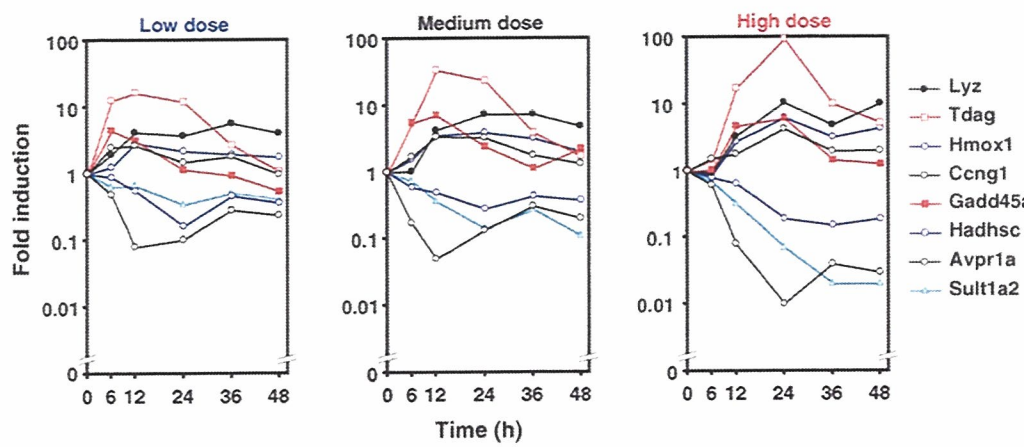

Fig. 6. Real-time RT-PCR analysis of the expression of the representative genes. Total RNA samples from four rats were pooled and used for real-time RT-PCR analysis. This figure shows the representative five up-regulated and three down-regulated genes as shown in Fig. 5. Official gene names are described in Fig. 5.

order to confirm the gene expression changes found in the DNA microarray analysis, real-time RT-PCR analysis was performed in eight representative genes (Fig. 6). The expression profiles and extent of these eight gene expressions were almost the same as those of the DNA microarray.

4. Discussion

Gene expression changes have been used to provide specific mechanistic information concerning the mode of action of toxicants. Toxicogenomics is an approach that applies microarray technology to toxicological evaluation paradigms. Toxicogenomic gene expression studies have been facilitated by the recent development of high-density microarrays.

In our previous study [16], the relationship between the hepatic gene expression profiles and hepatotoxicity was investigated in rats using in five typical hepatotoxicants. The mRNA of TA (400 mg/kg weight) administered rats was analyzed. Finally, 17 possible potential hepatotoxicity markers were proposed. In the present study, in order to evaluate the gene expression for hepatotoxicity in detail, we evaluated the effects of three dosages of TA, which causes zone-3 necrosis [17], by using a 9936 gene-spotted microarray slide. The dosage was selected according to a previous report [17]. The high-, medium-, low-dose administration was expected to cause severe toxicity, low toxicity and no toxicity, respectively. In this study, we compared between the extent of toxicity and the changes of gene expression in detail.

Previously, the effects of 300, 400 or 500 mg/kg weight of TA-administration in rats were reported [5,11,16]. The maximal point of TA toxicity estimated from the serum AST and ALT activities was 24 h after the administration. The present results were the same as those of previous reports. In the present study, the unconjugated bilirubin was not increased by TA-administration but the conjugated bilirubin was increased at 24 h by the high dosage of TA. These data confirmed that the toxicity model of TA-administration was successfully conducted in the present study. Additionally, the toxic time points of each dosage were estimated as 24 h.

Hierarchical clustering was performed to examine the gene expression data derived from the microarray analysis. All groups were extensively sorted into the early phase (6 and 12 h) or in the late phase (24, 36 and 48 h). In the early phase, the clusters were sorted in a time-dependent manner. Previously, Bulera et al. [18], reported in a comparison between low dose (40 mg/kg) and high dose (500 mg/kg) at early times (low dose: 3 and 6 h; high dose: 8 h) after the administration in rats using a microarray method, reported that all three groups were sorted into a the similar cluster. This result was similar to that of early phase in the present experiment (Fig. 2A). On the other hand, the late phase cluster was clustered in a dose-dependent manner (Fig. 2A). Therefore, we report here that the hierarchical clustering analysis demonstrated that the gene expression patterns were changed dose independently in the early phase of hepatotoxicity, but in dose dependently in the late phase of hepatotoxicity. Furthermore, hierarchical clustering at different dosages showed the same result as shown in Fig. 2B. The hierarchical distance between the early and the late phase were separated in a dose-dependent manner as shown by the dendrograms (Fig. 2B), suggesting that there was a certain relationship between the extent of hepatotoxicity and the gene expression pattern.

QT clustering based on the time after TA-administration was performed. This method can estimate the majority of gene expression profiles as previously reported [16]. As shown in Fig. 3, this result confirmed our finding from the hierarchical clustering analysis. Moreover, the hierarchical clustering and QT clustering based on the time after TA-administration also suggest that there was a dose dependency in the extent of the gene expression changes after the hepatotoxicity appeared.

QT clustering based on the TA dosage was also performed (Fig. 4). The profiles of both the average and median values from the QT clustering reflected the changes in biochemical markers. This result confirmed those of our previous study [16]. Furthermore, the present study indicated that the changes of the gene expression in the QT clustering became distinct in a dose-dependent manner. Taking these results into consideration, in this study, we demonstrated that the hepatic gene expression profiles are independent of the TA dosage and reflect the changes in the serum biochemical markers.

Category classification of the genes affected by TA-administration showed that the numbers of down-regulated genes were greater than those of the up-regulated genes, as reported previously [16].

Bulera et al. [18] reported the gene expression data after 24 h of TA-administration (500 mg/kg). In their study, expression changes were analyzed in 1600 genes and they showed that 133 genes were up-regulated and 163 genes were down-regulated. The microarray slides used in the present study spotted 49 of their 133 up-regulated genes (36.8%) and 68 of their 163 down-regulated genes (41.7%). In total, 117 of the 296 genes (39.5%) were spotted. In the present study, 39 of the 49 genes (79.6%) were up-regulated and 64 of the 68 genes (94.1%) were down-regulated (data not shown).

For example, FMO1, which metabolizes TA to a toxic metabolite, was down-regulated (<0.1-fold). In a total of 103 of 117 genes (88.0%), the expressions were similar to those reported by Bulera et al. [18].

In the previous study, using five traditional hepatotoxicants including TA we performed simultaneous measurements using other microarray slides (Rat Drug Response Chip, Hitachi) [16]. Most of the genes showed similar expression profiles to those of the present study. The expression profiles were confirmed in eight representative genes by real-time RT-PCR, which showed almost the same profile as that of the DNA microarray. This result suggested that our candidate genes could be sensitive markers for hepatotoxicity. However, the relationship between these genes was not clarified.

In summary, the present study demonstrated that there are distinct gene expression differences between pretoxic- and toxic-periods (Fig. 2), there is a dose dependency in the extent of the major gene expression changes after toxicity appears (Fig. 3), the major gene expression profiles reflect the biochemical marker activities (Fig. 4), and the candidate genes identified in our previous microarray analysis could be used as sensitive markers for hepatotoxicity (Fig. 5). In conclusion, the potential toxic effects appearing as gene expression changes are independent of the dosage of TA. The major gene expression profiles estimated by QT clustering analysis would be a sensitive marker for predicting potential hepatotoxicity.

Acknowledgements

This work was supported in part by a grant from the Ministry of Education, Science, Sports, and Culture of Japan, and by Research on Advanced Medical Technology, Health and Labor Science Research Grants from the Ministry of Health, Labor and Welfare of Japan. We thank Mr. Brent Bell for reviewing the manuscript.

References

[1] M. Bittner, P. Meltzer, J. Trent, Data analysis and integration: of steps and arrows, Nat. Genet. 22 (1999) 213–215.
[2] S. Tavazoie, J.D. Hughes, M.J. Campbell, R.J. Cho, G.M. Church, Systematic determination of genetic network architecture, Nat. Genet. 22 (1999) 281–285.
[3] L.J. Heyer, S. Kruglyak, S. Yooseph, Exploring expression data: identification and analysis of coexpressed genes, Genome Res. 11 (1999) 1106–1115.
[4] A.L. Hunter, M.A. Holscher, R.A. Neal, Thioacetamide-induced hepatic necrosis. I. Involvement of the mixed-function oxidase enzyme system, J. Pharmacol. Exp. Ther. 200 (1977) 439–448.
[5] T. Wang, K. Shankar, M.J. Ronis, H.M. Mehendale, Potentiation of thioacetamide liver injury in diabetic rats is due to induced CYP2E1, J. Pharmacol. Exp. Ther. 294 (2000) 473–479.
[6] M.C. Dyroff, R.A. Neal, Identification of the major protein adduct formed in rat liver after thioacetamide administration, Cancer Res. 41 (1981) 3430–3435.
[7] W.R. Porter, R.A. Neal, Metabolism of thioacetamide and thioacetamide *S*-oxide by rat liver microsomes, Drug Metab. Dispos. 6 (1978) 379–388.
[8] W.R. Porter, M.J. Gudzinowicz, R.A. Neal, Thioacetamide-induced hepatic necrosis. II. Pharmacokinetics of thioacetamide and thioacetamide *S*-oxide in the rat, J. Pharmacol. Exp. Ther. 208 (1979) 386–391.
[9] N. Sanz, C. Diez-Fernandez, A.M. Alvarez, L. Fernandez-Simon, M. Cascales, Age-related changes on parameters of experimentally induced liver injury and regeneration, Toxicol. Appl. Pharmacol. 154 (1999) 40–49.
[10] N. Sanz, C. Diez-Fernandez, D. Andres, M. Cascales, Hepatotoxicity and aging: endogenous antioxidant systems in hepatocytes from 2-, 6-, 12-, 18- and 30-month-old rats following a necrogenic dose of thioacetamide, Biochim. Biophys Acta 1587 (2002) 12–20.
[11] A. Zaragoza, D. Andres, D. Sarrion, M. Cascales, Potentiation of thioacetamide hepatotoxicity by phenobarbital pretreatment in rats. Inducibility of FAD monooxygenase system and age effect, Chem. Biol. Interact. 124 (2000) 87–101.
[12] A. Gozdz, E. Szczepanska-Sadowska, K. Szczepanska, W. Maslinski, B. Luszczyk, Vasopressin V1a, V1b and V2 receptors mRNA in the kidney and heart of the renin transgenic TGR(mRen2)27 and Sprague–Dawley rats, J. Physiol. Pharmacol. 53 (2002) 349–357.
[13] R.S. Ge, M.P. Hardy, Decreased cyclin A2 and increased cyclin G1 levels coincide with loss of proliferative capacity in rat Leydig cells during pubertal development, Endocrinology 138 (1997) 3719–3726.
[14] S.A. Shain, Exogenous fibroblast growth factors maintain viability, promote proliferation, and suppress GADD45alpha and GAS6 transcript content of prostate cancer cells genetically modified to lack endogenous FGF-2, Mol. Cancer Res. 2 (2004) 653–661.
[15] J.M. Rodriguez Parkitna, W. Bilecki, P. Mierzejewski, R. Stefanski, A. Ligeza, A. Bargiela, B. Ziolkowska, W. Kostowski, R. Przewlocki, Effects of morphine on gene expression in the rat amygdala, J. Neurochem. 91 (2004) 38–48.
[16] K. Minami, T. Saito, M. Narahara, H. Tomita, H. Kato, H. Sugiyama, M. Katoh, M. Nakajima, T. Yokoi, Relationship between hepatic gene expression profiles and hepatotoxicity in five typical hepatotoxicant-administered rats, Toxicol. Sci. 87 (2005) 296–305.
[17] H.J. Zimmerman, Hepatotoxicity: The Adverse Effects of Drugs and Other Chemicals on the Liver, 2nd ed., Lippncott Williams & Wilkins, Philadelphia, 1999, pp. 266–267.
[18] S.J. Bulera, S.M. Eddy, E. Ferguson, T.A. Jatkoe, J.F. Reindel, M.R. Bleavins, F.A. De La Iglesia, RNA expression in the early characterization of hepatotoxicants in Wistar rats by high-density DNA microarrays, Hepatology 33 (2001) 1239–1258.

J. Biochem. 139, 527–534 (2006)
doi:10.1093/jb/mvj055

Binding of Steroidogenic Factor-1 to the Regulatory Region Might Not Be Critical for Transcriptional Regulation of the Human *CYP1B1* Gene

Yuki Tsuchiya[1], Miki Nakajima[1], Shingo Takagi[1], Miki Katoh[1], Wenchao Zheng[2], Colin R Jefcoate[2] and Tsuyoshi Yokoi[1,*]

[1]Drug Metabolism and Toxicology, Division of Pharmaceutical Sciences, Graduate School of Medical Science, Kanazawa University, Kakuma-machi, Kanazawa 920-1192; and [2]Department of Pharmacology, Medical Science Center, University of Wisconsin, 1300 University Avenue, Madison, WI 53706, USA

Received November 18, 2005; accepted January 10, 2006

Cytochrome P450 (CYP) 1B1, which catalyzes 17β-estradiol 4-hydroxylation, is expressed in steroid-related tissues including ovary, testis, and adrenal gland. Generally, the expressions of steroidogenic CYPs are transcriptionally regulated by steroidogenic factor-1 (SF-1) and cAMP response element (CRE) binding protein (CREB). In the present study, we examined the possibility that the human *CYP1B1* gene might be regulated by SF-1 and CREB. Gel shift analyses revealed that *in vitro* translated SF-1 can bind to the putative SF-1 binding sites, SF-1a (at −1722) and SF-1b (at −2474), on the *CYP1B1* gene. *In vitro* translated CREB barely binds to the putative SF-1 binding sites. Luciferase analysis revealed that a reporter plasmid, pGL3 (−2623/+25), containing the SF-1a and SF-1b elements is transactivated by the concomitant co-expression of SF-1 and protein kinase A (PKA). However, the transcriptional activity is induced by PKA alone. Mutations in the SF-1a and SF-1b elements did not affect the luciferase activity. Thus, the binding of SF-1 to the putative SF-1 binding sites of the human *CYP1B1* gene might not be essential for transcriptional regulation. Interestingly, deletion and mutation analyses indicated that the PKA signaling pathway is involved in the xenobiotic responsive element (XRE)–mediated transactivation of the human *CYP1B1* gene.

Key words: CREB, CYP1B1, gene regulation, PKA; SF-1.

Abbreviations: AhR, aryl hydrocarbon receptor; ARNT, AhR nuclear translocator; CRE, cAMP response element; CREB, CRE binding protein; CYP, cytochrome P450; PKA, protein kinase A; SF-1, steroidogenic factor-1; TCDD, 2,3,7,8-tetrachlorodibenzo-*p*-dioxin; XRE, xenobiotic responsive element.

Cytochrome P450 (CYP)s comprise a multigene family of constitutive and inducible enzymes involved in the oxidative metabolic activation and detoxification of many endogenous and exogenous compounds (*1*, *2*). Human CYP1B1 is mainly expressed in lung, kidney, ovary, uterus, breast, prostate, and adrenal gland (*3*, *4*). Its function involves not only the metabolic activation of a variety of procarcinogens and promutagens, including polycyclic aromatic hydrocarbons (PAHs) and aryl amines (*4*), but also the hydroxylation of the endogenous substrate 17β-estradiol in human (*5*, *6*).

In rat, CYP1B1 expression has been reported to be increased by adrenocorticotropic hormone (ACTH) and cAMP (*7*, *8*). In addition, Zheng *et al.* (*9*, *10*) recently reported that the transcriptional regulation of the rat *CYP1B1* gene is mediated by steroidogenic factor-1 (SF-1) and cAMP response element binding protein (CREB). SF-1 is a member of the orphan nuclear receptor family. SF-1 is expressed in adrenal cortex, testis, ovary, pituitary gonadotrope cells, and hypothalamus (*11*, *12*), and is essential for adrenal development and sexual differentiation (*13*, *14*). SF-1 is activated by the cAMP-dependent protein kinase A (PKA) and plays an important role in regulating the expression of various steroidogenic genes, such as steroidogenic acute regulatory protein (*15*), CYP11A1 (*16*), CYP11B1 (*17*), CYP17 (*18*), and CYP19 (*19*). In the 5′-flanking region of these target genes, SF-1 binds to a consensus sequence (PuPuAGGTCA or PyCAAGGPyPy) as a monomer and enhances the transcriptional activation (*20*).

CREB is a member of the leucine zipper family, which is also activated by the PKA signaling pathway, and recognizes the cAMP response element (CRE) core sequence (TGACGTCA) of the target gene (*21*). SF-1 is involved in cAMP-regulated gene expression, since SF-1 interacts with CREB mediated by the PKA pathway (*22*, *23*).

In the rat *CYP1B1* gene, four SF-1 binding sites and two potential CREs have been identified at −5298 to −5110 (Far Upstream Enhancer Region, FUER) (*9*, *10*). Although the corresponding FUER rat homolog does not exist in the human *CYP1B1* gene, we found two putative SF-1 binding sites at −1722 and −2474 in the human *CYP1B1* gene. This prompted us to investigate the possibility that human CYP1B1 expressed in steroidogenic tissues might also be controlled by SF-1 and CREB. In the present study, we examined the binding of SF-1 or CREB to the putative SF-1 binding sites on the 5′-flanking region of the human *CYP1B1* gene by gel shift analyses. In addition,

*To whom all correspondence should be addressed. Tel/Fax: +81-76-234-4407, E-mail: TYOKOI@kenroku.kanazawa-u.ac.jp

luciferase analyses were performed using various reporter constructs containing the 5′-flanking region of the human *CYP1B1* gene to investigate the involvement of these factors in the transcriptional regulation.

MATERIALS AND METHODS

Chemicals and Reagents—The pGL3-basic plasmid and luciferase reporter assay system were from Promega (Madison, WI). The pCMV-CREB and pCMV-PKA plasmids, which contain the full-length cDNA of human CREB and the catalytic subunit of human PKA, respectively, were purchased from BD Biosciences Clontech (Palo Alto, CA). The pRc/RSV-SF-1 plasmid containing bovine SF-1 cDNA and rabbit anti–bovine SF-1 antiserum were kindly provided by Dr. Ken-Ichirou Morohashi (National Institute of Basic Biology, Okazaki, Japan). [γ-^{32}P]ATP was from Amersham (Buckinghamshire, UK). All primers and oligonucleotides were commercially synthesized by Hokkaido System Sciences (Sapporo, Japan). The mouse anti–human CREB monoclonal antibody was from Santa Cruz Biotechnology (Santa Cruz, CA). All other chemicals and solvents were of the highest grade commercially available.

In Vitro Transcription/translation and Gel Shift Analyses—One microgram of the pTNT-SF-1 plasmid and pTNT-CREB plasmid were incubated at 30°C for 90 min with the T7 TNT quick-coupled transcription/translation system (Promega) in the presence of methionine. The *in vitro* synthesized products were then subjected to gel shift analyses. Synthetic oligonucleotides were labeled with [γ-^{32}P]ATP using T4 polynucleotide kinase (Toyobo, Osaka, Japan). The oligonucleotide sequences are shown in Table 1. The sequence of the consensus SF-1 binding site (cSF) was from the bovine *CYP11B1* gene (*20*) and the sequence of the consensus cAMP response element (CRE) was provided by Santa Cruz Biotechnology. The reaction mixture contained 1 μl of the *in vitro* translated product, 2 μg of poly [dI-dC], 1 μg of salmon sperm DNA, and 30 fmol of radiolabeled probe (~20,000 cpm) with binding buffer [25 mM Hepes-KOH (pH 7.9), 0.5 mM EDTA, 50 mM KCl, 10% glycerol, 0.5 mM dithiothreitol, 0.5 mM (*p*-amidinophenyl) methanesulfonyl fluoride] in a final volume of 15 μl. The binding reaction was performed at 25°C for 30 min. To determine the specificity of the binding to the oligonucleotides, competition experiments were conducted by co-incubation with excess amounts of unlabeled competitors. For super-shift analyses, rabbit anti–bovine SF-1 antiserum or anti–human CREB monoclonal antibody were pre-incubated with the *in vitro* translated product on ice for 15 min, and then each radiolabeled probe was added. DNA-protein complexes were separated under nondenaturing conditions in 4% polyacrylamide gels with 0.5× TBE as the running buffer. The gels were dried, and then the DNA-protein complexes were detected and quantified with a Fuji Bio-Imaging Analyzer BAS 1000 (Fuji Film, Tokyo, Japan).

Plasmid Constructs—The pTNT-SF-1 plasmid was constructed by cloning the full-length bovine SF-1 cDNA digested with *Sac*II and *Xba*I from the pRc/RSV-SF-1 plasmid into the *Xho*I and *Xba*I-digested pTNT vector (Promega). The pTNT-CREB plasmid was constructed by cloning the full-length human CREB cDNA digested with *Eco*RI and *Mlu*I from the pCMV-CREB into the *Eco*RI and *Mlu*I-digested pTNT vector. A series of pGL3-basic plasmids containing the 5′-flanking region of the human *CYP1B1* gene (–2299/+25, –1652/+25, –1022/+25, –910/+25, and –732/+25) and mutated plasmids (–910/XRE3 mt, –910/XRE2 mt, and –910/Sp1-like mt) were constructed in our previous study (*24*). A plasmid containing the 5′-flanking region of the human *CYP1B1* from –2623 to +25 was constructed as follows: a DNA fragment containing the sequence from –2623 to –869 was amplified by PCR using the forward primer adapted to include a *Mlu*I site at the 5′ end, 5′-CGC GTA TCT AAG TTC CCC ATC ATG-3′, and the reverse primer, 5′-GAA AGT CGG CTC CAG TCA TAT CC-3′. After digestion with *Eco*RI, the PCR product was cloned into the *Mlu*I and *Eco*RI-digested pGL3-basic (–2299/+25) plasmid. The orientation of the construct was verified by restriction enzyme digestion or the nucleotide sequence was confirmed by DNA sequencing analysis. Mutated plasmids (–2623/SF-1a mt, –2623/SF-1b mt, and –2623/SF-1a/b mt) were constructed by site-directed mutagenesis with a QuikChange® site-directed mutagenesis kit (Stratagene, La Jolla, CA). For the –2623/SF-1a mt construct, the forward and reverse mutagenic primers were 5′-GGT CTC GAA CTC CTG AAA TCA AGT GAT CCG CCC GC-3′ and 5′-GCG GGC GGA TCA CTT GAT TTC AGG AGT TCG AGA CC-3′, respectively (mutated sites are underlined). For the –2623/SF-1b mt construct, the forward and reverse mutagenic primers were 5′-GGT GGA TCA CCT GAA ATC AGG AGT TTG AGA CCA GCC-3′ and 5′-GGC TGG TCT CAA ACT CCT GAT TTC AGG TGA TCC ACC-3′, respectively. Nucleotide sequences were confirmed by DNA sequencing analysis. The p0.2 plasmid containing the 0.2 kb proximal promoter region of the rat *CYP1B1* gene and the pFUER/0.2 plasmid containing the far upstream enhancer region (FUER) from –5298 to –5188 of the rat *CYP1B1* gene in addition to the 0.2 kb proximal promoter region were previously constructed (*9*).

Cells Culture and Luciferase Assay—The human ovarian granulosa–like tumor cell line KGN (*25*) and the mouse adrenal tumor cell line Y-1 were obtained from Riken Gene Bank (Tsukuba, Japan) and American Type Culture Collection (Rockville, MD), respectively. KGN cells were cultured in a 1:1 mixture of Dulbecco's modified Eagle's medium (DMEM) and Ham's F-12 medium (Nissui Pharmaceutical, Tokyo, Japan) supplemented with 10% (v/v) fetal bovine serum (FBS) (Invitrogen). Y-1 cells were cultured in DMEM supplemented with 10% FBS. These cells were maintained at 37°C under an atmosphere of 5% CO_2–95% air. For the luciferase assays, cells were seeded into 24-well plates (8×10^4 cells/well) and incubated for 24 h before transfection. KGN cells were transfected with 400 ng of *CYP1B1/luc* reporter gene plasmid and 50 ng of pRc/RSV-SF-1 plasmid or pRc/RSV vector in the presence of 50 ng of pCMV-PKA plasmid or pCMV vector using Superfect Transfect Regents (QIAGEN, Hilden, Germany) at a reagent:DNA ratio of 3:1 in 200 μl of serum-free culture medium. After incubation at 37°C for 3 h under an atmosphere of 5% CO_2–95% air, growth medium was added to the cells. Y-1 cells were transfected with the same plasmids as above using Tfx-20 reagent (Promega) at a reagent:DNA ratio of 2.5:1 in 200 μl of

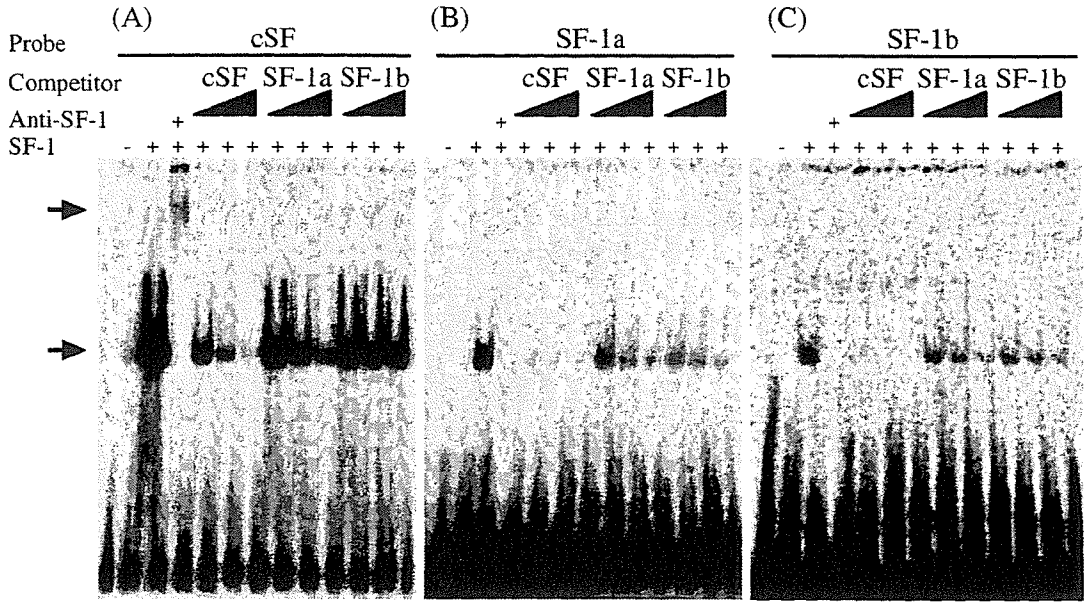

Fig. 1. **Gel shift analyses of the putative SF-1 binding sites on the human *CYP1B1* gene with SF-1.** Radiolabeled cSF (A), SF-1a (B), and SF-1b (C) were used as probes and each cold oligonucleotide was used as a competitor at 200-, 500-, and 1,000-fold molar excesses. For super-shift analyses, rabbit anti–bovine SF-1 serum was pre-incubated with *in vitro* translated SF-1 protein on ice for 15 min, and then the radiolabeled probe was added. DNA-protein complexes were separated under nondenaturing conditions in 4% polyacrylamide gels. The lower arrow indicates the position of the SF-1–dependent shifted band and the upper arrow indicates the super-shifted SF-1 complex.

serum-free culture medium. After incubation at 37°C for 1 h under an atmosphere of 5% CO_2–95% air, growth medium was added to the cells. After 48 h, the cells were resuspended in passive lysis buffer, and then the luciferase activity was measured with a luminometer (WALLAC, Turku, Finland) using a luciferase reporter assay system (Promega). Protein concentrations were determined using the Bradford protein assay regent (Bio-Rad, Hercules, CA) with bovine γ-globulin as the standard. The luciferase activity was normalized to the protein content.

Statistical Analyses—Data are expressed as mean ± SD of triplicate determinations. Statistical significance was determined by analysis of variance and Scheffe's test. A value of $P < 0.05$ was considered statistically significant.

RESULTS

Binding of SF-1 to the Putative SF-1 Binding Sites on the Human CYP1B1 Gene—A computer-assisted homology search revealed two putative SF-1 binding sites, SF-1a at –1722 and SF-1b at –2474, in the 5′-flanking region of the human *CYP1B1* gene. The SF-1a and SF-1b sequences are different from the consensus SF-1 binding sequence (PuPuAGGTCA) in one base. To determine whether SF-1 can bind to the SF-1a or SF-1b sequence on the human *CYP1B1* gene, gel shift analyses were performed (Fig. 1). Oligonucleotides used for the gel shift analyses are shown in Table 1. Using an oligonucleotide containing the consensus SF-1 binding sequence (cSF) as a probe, we confirmed that the *in vitro* translated SF-1 binds to cSF (Fig. 1A). A super-shifted band was observed with anti–SF-1 antiserum. However, the super-shifted band was not observed with normal rabbit IgG (data not shown). The band density was decreased by a cold cSF competitor. In contrast, the competition with the cold competitors of SF-1a and SF-1b was weak. Using SF-1a or SF-1b as a probe, the shifted band was also observed with SF-1, although the intensity was weak (Fig. 1, B and C). The shifted bands were abolished with anti–SF-1 antiserum, and excessive cold cSF competitors robustly diminished the DNA-protein complexes for SF-1a and SF-1b. In contrast, the competition with cold competitors of SF-1a and SF-1b was weak. These results indicate that SF-1 binds to the putative SF-1 binding sites on the human *CYP1B1* gene.

Table 1. **Oligoprobes used for gel shift analyses.**

Probe	Sequence	Position
SF-1a	5′-CGAACTCCTGACCTCAAGTGA-TCCGCCCGC-3′	–1737/–1708
SF-1b	5′-GTGGATCACCTGAGGTCAGGA-GTTTGAGAC-3′	–2491/–2462
cSF	5′-ACATACCCAAGGTCCCCTTT-3′	–337/–318
cCRE	5′-AGAGATTGCCTGACGTCAGA-GAGCTAG-3′	Artificial

Sequence and position of SF-1 binding sites in the human *CYP1B1* gene are listed. Each core region is underlined. SF-1a is actually the reverse complement of the SF-1 binding site. The consensus SF-1 binding site (cSF) sequence is that of the bovine *CYP11B1* gene. The consensus CRE (cCRE) sequence was created by Santa Cruz Biotechnology.

Binding of CREB to the Putative SF-1 Binding Sites on the Human CYP1B1 Gene—The sequences of SF-1a and SF-1b resemble that of the cAMP response element

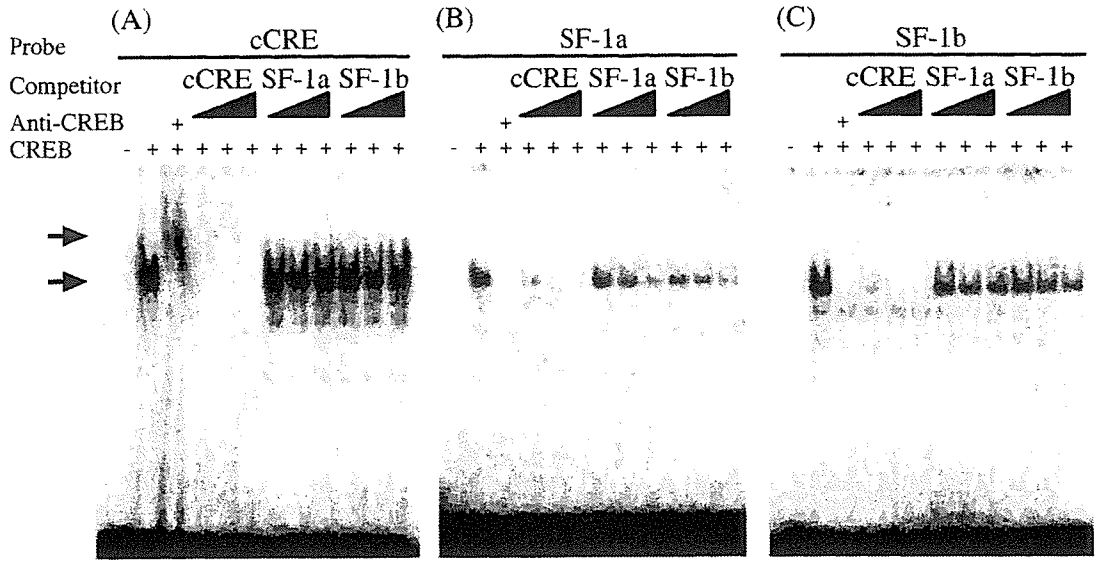

Fig. 2. **Gel shift analyses of the putative SF-1 binding sites on the human *CYP1B1* gene with CREB.** Radiolabeled cCRE (A), SF-1a (B), and SF-1b (C) were used as probes and each cold oligonucleotide was used as a competitor at 200-, 500-, and 1,000-fold molar excesses. For super-shift analyses, mouse anti-human CREB antibodies were pre-incubated with *in vitro* translated CREB protein on ice for 15 min, and then the radiolabeled probe was added. DNA-protein complexes were separated under nondenaturing conditions in 4% polyacrylamide gels. The lower arrow indicates the position of the CREB-dependent shifted band and the upper arrow indicates the super-shifted CREB complex.

(CRE: TGACGTCA), suggesting possible binding of CREB. To investigate whether CREB can bind to the SF-1a or SF-1b sites on the human *CYP1B1* gene, gel shift analyses were performed (Fig. 2). Using an oligonucleotide containing the consensus CRE sequence (cCRE), it was confirmed that the *in vitro* translated CREB binds to the sequence (Fig. 2A). A super-shifted band was observed with anti-CREB antibody. In contrast, no super-shifted band was observed with normal mouse IgG (data not shown). The band was competed out by cCRE when used as a cold competitor, but not by cold competitors of SF-1a and SF-1b. Using SF-1a or SF-1b as a probe, a shifted band was also observed with CREB (Figs. 2B and 2C). The shifted band was abolished with anti-CREB antibody, although no super-shifted band was observed. Thus, CREB barely binds to the putative SF-1–binding sites on the human *CYP1B1* gene.

Transcriptional Activities of the Human CYP1B1 Gene with the Co-Expression of SF-1 and PKA in KGN Cells—SF-1–dependent transcriptional regulation is known to be activated by PKA. To investigate whether SF-1 is involved in the transcriptional activation of the human *CYP1B1* gene via the putative SF-1 binding sites, luciferase assays were performed (Fig. 3). A luciferase reporter plasmid containing the 5′-flanking region from –2623 to +25 of the human *CYP1B1* gene was transiently transfected into KGN cells co-transfected with pRc/RSV-SF-1 plasmid, pCMV-PKA plasmid or in combination. Although the transcriptional activity was not affected by the co-expression of SF-1, it was significantly (5.9-fold) increased by the concomitant co-expression of SF-1 and PKA. However, the co-expression of PKA alone also produced similar transcriptional activation (6.7-fold). Using the mutated plasmids pGL3 (–2623/SF-1a mt), pGL3 (–2623/SF-1b mt), and pGL3 (–2623/SF-1a/b mt), the role of the putative SF-1 binding sites in the transcriptional activities was determined. The mutations did not affect the transcriptional activities in either the basal or PKA-dependent activities. These results suggest that the SF-1a and SF-1b sequences do not function in the transcriptional regulation of the human *CYP1B1* gene.

A series of deleted pGL3 plasmids were transfected into KGN cells co-transfected with the SF-1–expression vector in the absence or presence of the PKA-expression vector (Fig. 3). Using the pGL3 (–1652/+25), pGL3 (–1022/+25), and pGL3 (–910/+25) plasmids, stimulation of the transcriptional activities by PKA was observed in each plasmid (6.0-, 4.0-, and 4.9-fold, respectively), although no effects of the co-expression of SF-1 were observed (Fig. 3). Further deletion to –732 abolished the PKA-dependent transactivation. When CREB was co-expressed instead of SF-1 for each reporter construct, similar results were obtained (data not shown). These results suggest that the transcription of the human *CYP1B1* gene is regulated by PKA in the region –910 to–732.

Comparison of KGN Cells and Y-1 Cells in the Transcriptional Activities of the CYP1B1 Gene with the Co-Expression of SF-1 and PKA—As described above, SF-1 failed to transactivate the human *CYP1B1* gene. To investigate the responsiveness of SF-1 in KGN cells, a reporter plasmid containing the enhancer region of the rat *CYP1B1* gene (pFUER/0.2), which is known to be transactivated by SF-1 (*10*), was transfected (Fig. 4A). In contrast to the plasmids containing the human *CYP1B1* gene, the reporter activity of pFUER/0.2 was slightly increased by the co-expression of SF-1 (7.1-fold). Furthermore, the concomitant co-expression of SF-1 and PKA produced a maximum

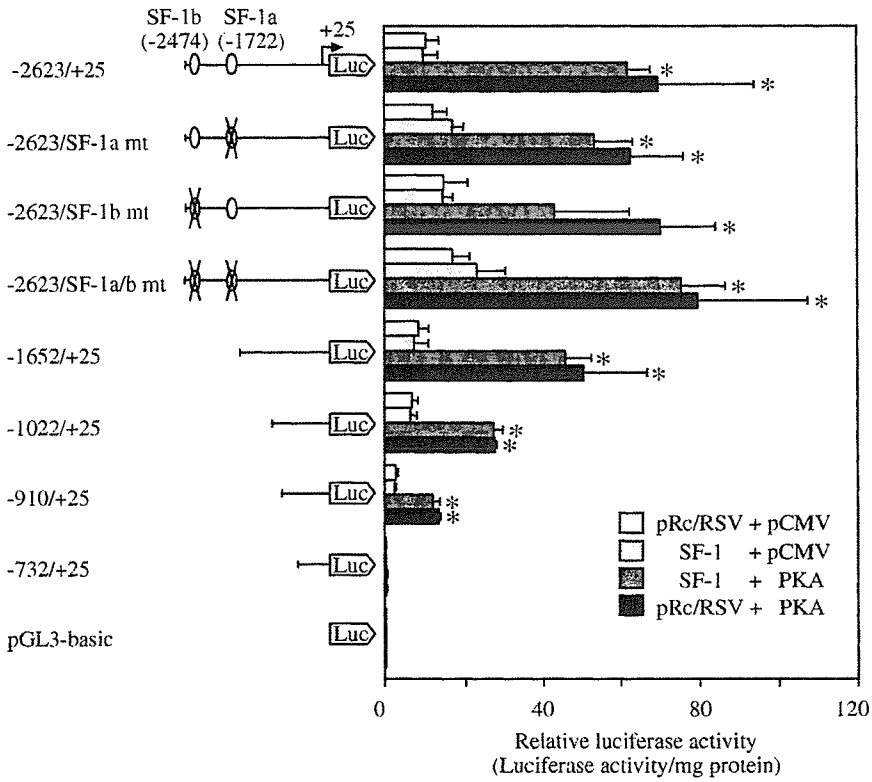

Fig. 3. **Transcriptional activity of the human *CYP1B1* gene in KGN cells.** A series of reporter constructs containing the 5′-flanking region of the human *CYP1B1* gene were transiently transfected into KGN cells with pRc/RSV-SF-1 plasmid (SF-1), pCMV-PKA plasmid (PKA), or in combination. To adjust the total amount of transfected plasmid, an empty vector (pRc/RSV or pCMV) was transfected as a control. After 48 h, luciferase activity and protein content were determined for the harvested cellular extracts. Relative luciferase activities are expressed as luciferase activity per mg protein. Each column represents the mean ± SD of three independent experiments $^*P < 0.05$, compared with control (pRc/RSV and pCMV vector co-transfection).

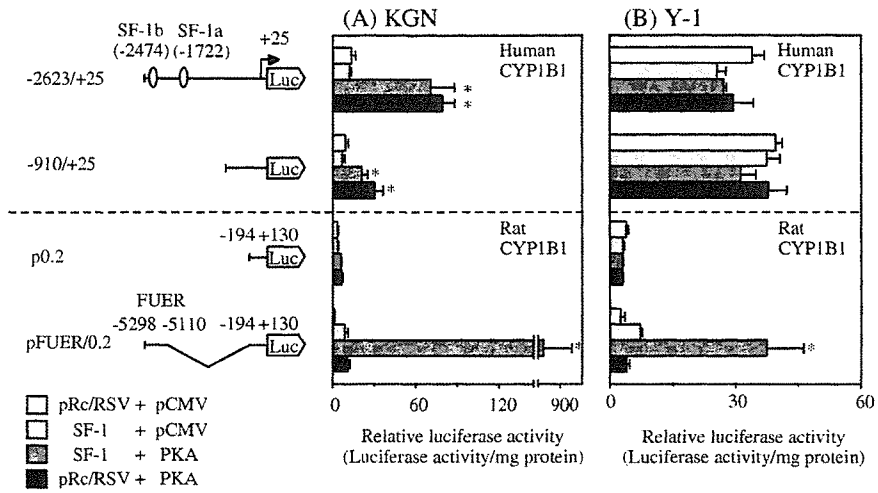

Fig. 4. **Transcriptional activity of the human or rat *CYP1B1* gene in KGN or Y-1 cells.** The reporter plasmids were pGL3 (–2623/+25) and pGL3 (–910/+25) containing the 5′-flanking region of the human *CYP1B1* gene, as well as pFUER/0.2 and p0.2 containing the 5′-flanking region of the rat *CYP1B1* gene. These reporter plasmids were transiently transfected into KGN cells (A) and Y-1 cells (B) with pRc/RSV-SF-1 plasmid (SF-1), pCMV-PKA plasmid (PKA), or in combination. To adjust the total amount of transfected plasmid, an empty vector (pRc/RSV or pCMV) was transfected as a control. After 48 h, the luciferase activity and protein content were determined for the harvested cellular extracts. Relative luciferase activities are expressed as luciferase activity per mg protein. Each column represents the mean ± SD of three independent experiments $^*P < 0.05$, compared with control (pRc/RSV and pCMV vector co-transfection).

transcriptional activation of 697-fold. The reporter activity of the p0.2 construct was not affected by the co-expression of SF-1. These results suggest that SF-1 can function in KGN cells.

Mouse adrenal tumor Y-1 cells are frequently used for the examination of SF-1–regulated transactivation of target genes. Therefore, the SF-1-dependent transactivation of the human *CYP1B1* gene was investigated using Y-1

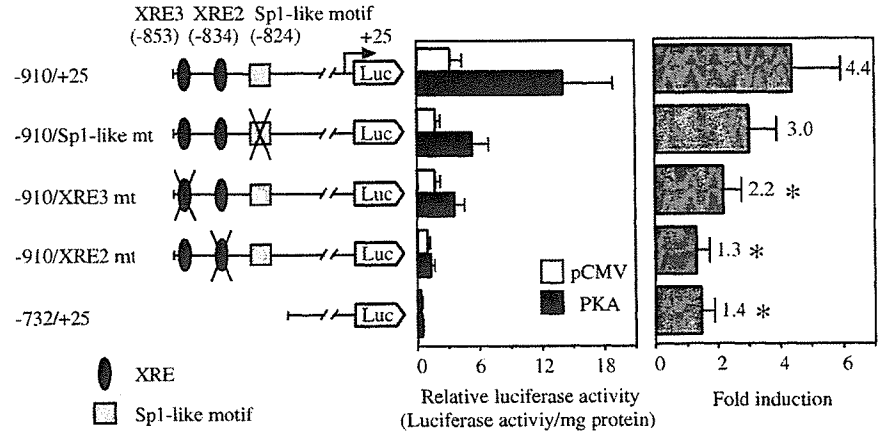

Fig. 5. **Effects of mutations of XRE3, XRE2, and the Sp1-like motif in the 5′-flanking region of the human *CYP1B1* gene on the transcriptional activity by PKA.** A series of reporter plasmids were transiently transfected into KGN cells with the pCMV-PKA plasmids. To adjust the total amount of transfected plasmid, the pCMV vector was transfected as a control. After 48 h, the luciferase activity and protein content were determined for the harvested cellular extracts. Relative luciferase activities are expressed as luciferase activity per mg protein. Constitutive and PKA-inducible transcriptional activities were demonstrated (left panel), and fold induction by PKA over control in each reporter construct was demonstrated (right panel). Each column represents the mean ± SD of three independent experiments $^*P < 0.05$, compared with pGL3 (–910/+25).

cells (Fig. 4B). In accordance with the previous report (*10*), the reporter activity of pFUER was increased by the co-expression of SF-1 (2.9-fold) and concomitant co-expression of SF-1 and PKA (15-fold). In contrast, reporter plasmids containing the human *CYP1B1* gene were not transactivated by the co-expression SF-1 or PKA in Y-1 cells. These results suggest that the regulation of the rat and human *CYP1B1* genes by SF-1 is not similar.

PKA-Dependent Transactivation Is Mediated by XRE— The *CYP1B1* gene is well known to be regulated by a ligand-activated aryl hydrocarbon receptor (AhR) *via* the xenobiotic responsive element (XRE). In our previous study (*24*), it was demonstrated that two XRE sequences at –853 and –834 on the 5′-flanking region of *CYP1B1* gene cooperatively regulate the constitutive and ligand-inducible transcriptional regulation of *hCYP1B1* with the Sp1-like motif at –824. To examine the possibility that the PKA-dependent transactivation is associated with these elements, luciferase analyses with mutated reporter constructs were performed (Fig. 5). The constitutive activities of the mutated reporter plasmids pGL3 (–910/Sp1-like mt), pGL3 (–910/XRE3 mt), and pGL3 (–910/XRE2 mt) were 56%, 52%, and 30% that of wild-type pGL3 (–910/+25), respectively. The reporter activities of pGL3 (–910/+25) and pGL3 (–910/Sp1-like mt) were induced 4.4-fold and 3.0-fold by the co-transfection of PKA, respectively. In contrast, mutations in XRE3 and XRE2 significantly reduced the PKA-dependent transactivation to 2.2-fold and 1.3-fold, respectively, and the PKA-dependent transactivation was not observed with the pGL3 (–732/+25) plasmid (1.4-fold). These results suggest that the PKA-dependent transcription of the human *CYP1B1* gene is mediated by XRE3 and XRE2.

DISCUSSION

Steroidogenic CYPs such as CYP11A1 (*16*), CYP11B1 (*17*), CYP17 (*18*), and CYP19 (*19*) possess a common cAMP responsive enhancer region in the 5′-flanking region of the genes. These are regulated by SF-1 and/or CREB (*26*). It has been reported that PKA directly phosphorylates SF-1 (*27*). It was recently reported that PKA phosphorylates mitogen-activated protein kinase phosphatase-1 (MKP-1), which dephosphorylates SF-1 (*28*). Although the functions of the phosphorylation and/or dephosphorylation of SF-1 are controversial, the involvement of PKA in the activation of SF-1 would be plausible. CREB can bind to the target gene after the phosphorylation by PKA, which is activated by cAMP (*29*). CYP1B1 is also highly expressed in steroidogenic tissues such as ovary and adrenal gland, and acts in the metabolism of 17β-estradiol. It has been reported that rat CYP1B1 is regulated by SF-1 and CREB (*9*, *10*). In the present study, we investigated the possibility that SF-1 or CREB might be involved in the transcriptional regulation of the human *CYP1B1* gene.

The binding of SF-1 and CREB to two SF-1 binding sites (SF-1a and SF-1b) on the human *CYP1B1* gene was demonstrated by gel shift analyses. However, luciferase analyses revealed no transactivation of the human *CYP1B1* gene with SF-1. A similar phenomenon has been reported for human CYP11B2, aldosterone synthase, expressed in adrenal zona glomerulosa (*30*). Although SF-1 binds to the Ad4 sequence on the promoter region of the *CYP11B2* gene, SF-1 does not stimulate the transcriptional activity. Thus, if the binding affinity of SF-1 and CREB to DNA is low, these factors might be unable to transactivate.

In the rat *CYP1B1* gene, two potential CREs to which CREB can bind were identified at –5122 and –5255 (*9*). Furthermore, four SF-1 binding elements to which SF-1 can bind were identified at –5298 to –5110 (Far Upstream Enhancer Region, FUER) of the rat *CYP1B1* gene (*10*). Zheng and Jefcoate (*10*) also reported that SF-1 and CREB cooperatively transactivate the rat *CYP1B1* gene. In the present study, the SF-1– and PKA-dependent transactivation of the rat *CYP1B1* gene, but not the human *CYP1B1* gene, was observed in both KGN cells and Y-1

cells. When the sequences of the human and rat *CYP1B1* genes are compared, the homology is greater than 90% in the 5′-flanking region −1058 to −802 containing XRE. Since both the human and rat *CYP1B1* genes are up-regulated by AhR *via* XRE, this region is critical for human and rat *CYP1B1* gene regulation. However, far from −1 kbp in the 5′-flanking region, the homology between the human and rat *CYP1B1* genes decreases prominently, and the corresponding FUER rat homolog (−5298/−5110) is not found in the human *CYP1B1* gene. In the present study, we focused on two putative SF-1 binding sites at −1722 and −2474 in the *hCYP1B1* gene. Although rat FUER has multiple binding regions for SF-1 and CREB in a short sequence (189 bp), the SF-1a and SF-1b sites in the human *CYP1B1* gene exist separately. Thus, the dissimilarity in the sequences in the regulatory regions of the human and rat *CYP1B1* genes might be the cause of the low contribution of SF-1 to the regulation of the human *CYP1B1* gene. Taking our present data into consideration, SF-1 would not be a major regulator of human CYP1B1 expression. However, we cannot exclude the possibility that SF-1 might act indirectly if SF-1 modifies another transcriptional factor(s) that regulates human CYP1B1.

We found that PKA activates the transcription between −910 to −732 on the 5′-flanking region of the human *CYP1B1* gene (Fig. 3). This region includes two XRE sites and an Sp1-like motif, which play roles in the regulation of *CYP1B1* in constitutive and AhR-ligand dependent expression (*24*). It is well known that AhR binds to XRE after heterodimerization with AhR nuclear translocator (ARNT) (*31*, *32*). Interestingly, mutations in XRE3 at −853 and XRE2 at −834 inhibit the PKA-dependent activation (Fig. 5). As shown in Fig. 4, this PKA-dependent transactivation of the human *CYP1B1* gene was observed in KGN cells, but not in Y-1 cells. In KGN cells, AhR mRNA is expressed and can induce the CYP1B1 mRNA in the presence of ligands (data not shown). In contrast, AhR mRNA is not expressed in Y-1 cells (*9*). Thus, AhR is likely to be involved in PKA-dependent transactivation. A number of early studies reported the phosphorylation of AhR; especially, the phosphorylation of AhR via protein kinase C (PKC) is well known to be essential for the binding of AhR to XRE (*33*, *34*). Until now, the association of PKA with the phosphorylation of AhR activation was unknown. However, it has been reported that PKA augments the transactivation potential of ARNT, a partner of AhR (*35*). The findings of our study suggest that the PKA signaling pathway is partially involved in the transcriptional regulation of the human *CYP1B1* gene *via* XRE, although further studies are necessary.

In conclusion, we demonstrated the binding of SF-1 and CREB to the putative SF-1 binding sites of the human *CYP1B1* gene, but these factors do not activate transcription. Thus, SF-1 and CREB might not be essential for the regulation of the human *CYP1B1* gene. Interestingly, it was found that PKA signaling is involved in the XRE-mediated transactivation in the human *CYP1B1* gene.

We are grateful to Dr. Ken-ichirou Morohashi of the National Institute for Basic Biology (Okazaki, Japan) for providing the pRc/RSV-SF-1 plasmid and anti–SF-1 serum. We also thank Drs. Yoshihiro Nishi, Toshihiko Yanase, and Hajime Nawata of Kyushu University (Fukuoka, Japan) for providing the KGN cells. We acknowledge Mr. Brent Bell for reviewing the manuscript. This work was supported in part by Research on Advanced Medical Technology, Health and Labor Science Research Grants from the Ministry of Health, Labor and Welfare of Japan.

REFERENCES

1. Gonzalez, F.J. (1988) The molecular biology of cytochrome P450s. *Pharmacol. Rev.* **40**, 243–288
2. Guengerich, F.P. and Shimada, T. (1991) Oxidation of toxic and carcinogenic chemicals by human cytochrome P-450 enzymes. *Chem. Res. Toxicol.* **4**, 391–407
3. Sutter, T.R., Tang, Y.M., Hayes, C.L., Wo, Y-Y.P., Jabs, E.W., Li, X., Yin, H., Cody, C.W., and Greenlee, W.F. (1994) Complete cDNA sequence of a human dioxin-inducible mRNA identifies a new gene subfamily of cytochrome P450 that maps to chromosome 2. *J. Biol. Chem.* **269**, 13092–13099
4. Shimada, T., Hayes, C.L., Yamazaki, H., Amin, S., Hecht, S.S., Guengerich, F.P., and Sutter, T.R. (1996) Activation of chemically diverse procarcinogens by human cytochrome P450 1B1. *Cancer Res.* **56**, 2979–2984
5. Hayes, C., Spink, D., Spink, B., Cao, J., Walker, N., and Sutter, T. (1996) 17β-Estradiol hydroxylation catalyzed by human cytochrome P450 1B1. *Proc. Natl. Acad. Sci. USA* **93**, 9776–9781
6. Spink, D.C., Spink, B.C., Cao, J.Q., Gierthy, J.F., Hayes, C.L., Li, Y., and Sutter, T.R. (1997) Induction of cytochrome P450 1B1 and catechol estrogen metabolism in ACHN human renal adenocarcinoma cells. *J. Steroid. Biochem. Mol. Biol.* **62**, 223–232
7. Bhattacharyya, K.K., Brake, P.B., Eltom, S.E., Otto, S.A., and Jefcoate, C.R. (1995) Identification of a rat adrenal cytochrome P450 active in polycyclic hydrocarbon metabolism as rat CYP1B1. Demonstration of a unique tissue-specific pattern of hormonal and aryl hydrocarbon receptor-linked regulation. *J. Biol. Chem.* **270**, 11595–11602
8. Brake, P.B. and Jefcoate, C.R. (1995) Regulation of cytochrome P4501B1 in cultured rat adrenocortical cells by cyclic adenosine 3′,5′-monophosphate and 2,3,7,8-tetrachlorodibenzo-*p*-dioxin. *Endocrinology* **136**, 5034–5041
9. Zheng, W., Brake, P.B., Bhattacharyya, K.K., Zhang, L., Zhao, D., and Jefcoate, C.R. (2003) Cell selective cAMP induction of rat *CYP1B1* in adrenal and testis cells. Identification of a novel cAMP-responsive far upstream enhancer and a second Ah receptor-dependent mechanism. *Arch. Biochem. Biophys.* **416**, 53–67
10. Zheng, W. and Jefcoate, C.R. (2005) Steroidogenic factor-1 interacts with cAMP response element-binding protein to mediate cAMP stimulation of *CYP1B1* via a far upstream enhancer. *Mol. Pharmacol.* **67**, 499–512
11. Ikeda, Y., Lala, D.S., Luo, X., Kim, E., Moisan, M.P., and Parker, K.L. (1993) Characterization of the mouse FTZ-F1 gene, which encodes a key regulator of steroid hydroxylase gene expression. *Mol. Endocrinol.* **7**, 852–860
12. Morohashi, Ki. (1999) Gonadal and extragonadal functions of Ad4BP/SF-1: developmental aspects. *Trends Endocrinol. Metab.* **10**, 169–173
13. Luo, X., Ikeda, Y., Lala, D.S., Baity, L.A., Meade, J.C., and Parker, K.L. (1995) A cell-specific nuclear receptor plays essential roles in adrenal and gonadal development. *Endocr. Res.* **21**, 517–524
14. Luo, X., Ikeda, Y., Parker, K.L. (1994) A cell-specific nuclear receptor is essential for adrenal and gonadal development and sexual differentiation. *Cell* **77**, 481–490
15. Sugawara, T., Holt, J.A., Kiriakidou, M., and Strauss III, J.F. (1996) Steroidogenic factor 1-dependent promoter activity of the human steroidogenic acute regulatory protein (StAR) gene. *Biochemistry* **35**, 9052–9059

16. Hu, M.C., Hsu, N.C., Pai, C.I., Wang, C.K., and Chung, B.C. (2001) Functions of the upstream and proximal steroidogenic factor 1 (SF-1)-binding sites in the *CYP11A1* promoter in basal transcription and hormonal response. *Mol. Endocrinol.* **15**, 812–818
17. Wang, X.L., Bassett, M., Zhang, Y., Yin, S., Clyne, C., White, P.C., and Rainey, W.E. (2000) Transcriptional regulation of human 11β-hydroxylase (*hCYP11B1*). *Endocrinology* **141**, 3587–3594
18. Hanley, N.A., Rainey, W.E., Wilson, D.I., Ball, S.G., and Parker, K.L. (2001) Expression profiles of SF-1, DAX1, and CYP17 in the human fetal adrenal gland: potential interactions in gene regulation. *Mol. Endocrinol.* **15**, 57–68
19. Michael, M.D., Kilgore, M.W., Morohashi, K., and Simpson, E.R. (1995) Ad4BP/SF-1 regulates cyclic AMP-induced transcription from the proximal promoter (PII) of the human aromatase P450 (*CYP19*) gene in the ovary. *J. Biol. Chem.* **270**, 13561–13566
20. Morohashi, K., Honda, S., Inomata, Y., Handa, H., and Omura, T. (1992) A common *trans*-acting factor, Ad4-binding protein, to the promoters of steroidogenic P-450s. *J. Biol. Chem.* **267**, 17913–17919
21. Andrisani, O.M., (1999) CREB-mediated transcriptional control. *Crit. Rev. Eukaryot. Gene Expr.* **9**, 19–32
22. Ito, M., Park, Y., Weck, J., Mayo, K.E., and Jameson, J.L. (2000) Synergistic activation of the inhibin α-promoter by steroidogenic factor-1 and cyclic adenosine 3′,5′-monophosphate. *Mol. Endocrinol.* **14**, 66–81
23. Yazawa, T., Mizutani, T., Yamada, K., Kawata, H., Sekiguchi, T., Yoshino, M., Kajitani, T., Shou, Z., and Miyamoto, K. (2003) Involvement of cyclic adenosine 5′-monophosphate response element-binding protein, steroidogenic factor 1, and Dax-1 in the regulation of gonadotropin-inducible ovarian transcription factor 1 gene expression by follicle-stimulating hormone in ovarian granulosa cells. *Endocrinology* ***144***, *1920–1930*
24. Tsuchiya, Y., Nakajima, M., and Yokoi, T. (2003) Critical enhancer region to which AhR/ARNT and Sp1 bind in the human *CYP1B1* gene. *J. Biochem.* **133**, 583–592
25. Nishi, Y., Yanase, T., Mu, Y., Oba, K., Ichino, I., Saito, M., Nomura, M., Mukasa, C., Okabe, T., Goto, K., Takayanagi, R., Kashimura, Y., Haji, M., and Nawata, H. (2001) Establishment and characterization of a steroidogenic human granulosa-like tumor cell line, KGN, that expresses functional follicle-stimulating hormone receptor. *Endocrinology* **142**, 437–445
26. Val, P., Lefrancois-Martinez, A.M., Veyssiere, G., and Martinez, A. (2003) SF-1 a key player in the development and differentiation of steroidogenic tissues. *Nucl. Recept.* **1**, 8
27. Zhang, P. and Mellon, S.H. (1996) The orphan nuclear receptor steroidogenic factor-1 regulates the cyclic adenosine 3′,5′-monophosphate-mediated transcriptional activation of rat cytochrome P450c17 (17α-hydroxylase/c17–20 lyase). *Mol. Endocrinol.* **10**, 147–158
28. Sewer, M.B. and Waterman, M.R. (2003) cAMP-dependent protein kinase enhances CYP17 transcription via MKP-1 activation in H295R human adrenocortical cells. *J. Biol. Chem.* **278**, 8106–8111
29. Don, J. and Stelzer, G. (2002) The expanding family of CREB/CREM transcription factors that are involved with spermatogenesis. *Mol. Cell. Endocrinol.* **187**, 115–124
30. Bassett, M.H., Zhang, Y., Clyne, C., White, P.C., and Rainey, W.E. (2002) Differential regulation of aldosterone synthase and 11β-hydroxylase transcription by steroidogenic factor-1. *J. Mol. Endocrinol.* **28**, 125–135
31. Hankinson, O. (1995) The aryl hydrocarbon receptor complex. Annu. *Rev. Pharmacol. Toxicol.* **35**, 307–340
32. Schmidt, J.V. and Bradfield, C.A. (1996) Ah receptor signaling pathways. *Annu. Rev. Cell. Biol.* **12**, 55–89
33. Berghard, A., Gradin, K., Pongratz, I., Whitelaw, M., and Poellinger, L. (1993) Cross-coupling of signal transduction pathways: the dioxin receptor mediates induction of cytochrome P-450IA1 expression via a protein kinase C-dependent mechanism. *Mol. Cell. Biol.* **13**, 677–689
34. Long, W.P., Pray-Grant, M., Tsai, J.C., and Perdew, G.H. (1998) Protein kinase C activity is required for aryl hydrocarbon receptor pathway-mediated signal transduction. *Mol. Pharmacol.* **53**, 691–700
35. Long, W.P., Chen, X., and Perdew, G.H. (1999) Protein kinase C modulates aryl hydrocarbon receptor nuclear translocator protein-mediated transactivation potential in a dimer context. *J. Biol. Chem.* **274**, 12391–12400